Synthesis of nitrogen-doped carbon with three-dimensional mesostructures for CO_2 capture

Manli Yao · Lin Wang · Xin Hu · Gengshen Hu · Mengfei Luo · Maohong Fan

Abstract The objective of this research was to develop a new CO_2 sorbent, three-dimensional nitrogen-doped mesoporous carbon (KIT-6-CN). KIT-6-CN was synthesized by nano-replication using carbon tetrachloride and ethylenediamine as precursors, and KIT-6 with cubic *Ia3d* symmetry as a hard template. The new CO_2 sorbent has a relatively high BET surface area of 587 m^2/g, a high pore volume of 0.91 cm^3/g, and the mesostructures with pore diameters centered at 1.7 and 6.3 nm. The transmission electron microscopy of the KIT-6-CN shows that after removal of silica by NaOH, KIT-6-CN possesses three-dimensional mesoporous structure. CO_2 adsorption–desorption isotherms indicate that this nitrogen-doped material has relatively high CO_2 capture capacities of 2.11 mmol/g at 25 °C and 3.09 mmol/g at 0 °C, which are superior to those of the pure carbon material (KIT-6-C) with analogous mesostructures. Cyclic CO_2 sorption–desorption tests demonstrated the stability of the sorbent. Thus, the new sorbent can potentially be a good candidate for CO_2 capture.

M. Yao · L. Wang · G. Hu (✉) · M. Luo
Key Laboratory of the Ministry of Education for Advanced Catalysis Materials, Institute of Physical Chemistry, Zhejiang Normal University, Jinhua 321004, People's Republic of China
e-mail: gshu@zjnu.edu.cn

X. Hu
College of Chemistry and Life Sciences, Zhejiang Normal University, Jinhua 321004, People's Republic of China

M. Fan (✉)
Department of Chemical and Petroleum Engineering, University of Wyoming, Laramie, WY 82071, USA
e-mail: mfan@uwyo.edu

Introduction

In the recent decades, carbon dioxide is gradually recognized as the most important anthropogenic greenhouse gas (GHG) leading to global warming [1–8], so the removal of CO_2 from industrial flue gas has become an important issue [2, 9]. Carbon materials were considered as potential candidates for CO_2 capture because the weak interaction between CO_2 and carbon requires lower-energy requirements with respect to other sorbents, such as zeolites.

In recent years, research people paid much attention to the ordered mesoporous carbon materials [10–14], because of their advantages of separation, adsorption, catalysis of large molecules, and energy storage. There are many ways to synthesize ordered mesoporous carbon materials [13–17]. For example, the soft-template method as a facile route has been applied to fabricate mesoporous carbon very recently. In another way, Vinu et al. [18] successfully reported the preparation of mesoporous carbon nitride (C_3N_4) with an uniform pore-size distribution using SBA-15 as a template. In another study, Deng et al. synthesized mesoporous carbon nitride using SBA-15 as hard template for CO_2 capture [19]. It is popular and viable to synthesize porous carbons adopting the ordered mesoporous silicas as the hard templates, since the pore structure and the textural parameters of mesoporous silica materials can be easily controlled by many methods. It is well known that three-dimensional (3D) pore channels are more advantageous for mass diffusion than 2D pores. Unfortunately, the synthesis of 3D nitrogen-doped mesoporous carbon has rarely been reported.

In this work, 3D-ordered nitrogen-doped mesoporous carbon was synthesized using 3D mesoporous silica KIT-6 as the hard template and ethylenediamine (EDA) as the nitrogen source. Compared with undoped mesoporous carbon, the nitrogen-doped mesoporous carbon shows better CO_2 adsorption performance.

Experimental

Chemicals

All chemicals were used as received from the chemical vendors without further purification. Triblock copolymer poly (ethylene oxide)-b-poly (propylene oxide)-b-poly (ethylene oxide) (Pluronic P123, EO_{20}-PO_{70}-EO_{20}, Mw = 5800 g/mol) and EDA were purchased from Sigma-Aldrich. Butanol, carbon tetrachloride (CTC), tetraethyl orthosilicate (TEOS) and sucrose were obtained from Quzhou Reagent. Pure N_2 and 10 % CO_2/N_2 gases were obtained from Jinhua Gas. Distilled water was used in all experiments.

Synthesis

Preparation of the KIT-6 silica template

Mesoporous silica KIT-6 was synthesized following the procedures available in the literature by Ryong Ryoo [20]. In a typical synthesis batch, a homogeneous solution was obtained by dissolving 6.0 g of P123 in 217 g of distilled water and 11.8 g of concentrated HCl solution (35 wt%). To this solution, 6 g of butanol was added under stirring at 35 °C for an hour, followed by slow addition of 12.9 g of TEOS. The mixture was kept under magnetic stirring for 24 h at 35 °C, and subsequently heated to 100 °C for 24 h under static conditions in a teflon-lined autoclave. The solid product was filtered and washed to neutral with extensive deionized water, and then the sample was dried at room temperature overnight. The final material was obtained by calcinations at 550 °C (heating rate 5 °C/min) for 5 h to remove the P123 template in air.

Synthesis of nitrogen-doped mesoporous carbon material

The nitrogen-doped mesoporous carbon material was synthesized according to the route reported by Li [21] and Deng [19]. The difference is that 3D-ordered mesoporous silica KIT-6 rather was used as a hard template in this study with the aim to synthesize mesoporous carbon with 3D structure. In the typical procedure, 0.5 g of the silica KIT-6 template was added to a mixed solution containing 1.1 mL EDA and 1.3 g of CTC at room temperature. Then, the

above solution was heated at 90 °C for 6 h with stirring under reflux to induce polymerization of the precursor. The resulting dark-brown mixture was pre-pyrolyzed at 400 °C for 2 h in a helium atmosphere. The pyrolyzed sample was refilled with 0.75 mL EDA and 0.8 mL of CTC at 90 °C. After pyrolysis at 600 °C for 5 h in helium, the final mesoporous carbon product was obtained by using 2 mol/L NaOH aqueous solution to remove the silica template from the carbon–silica composite.

Synthesis of mesoporous carbon materials

For comparison, the mesoporous carbon materials were synthesized mainly according to the procedures available in the literature [10]. 1.25 g sucrose as the carbon source was dissolved in mixture solution containing 5 mL distilled water and 80 uL H_2SO_4, and then 1 g KIT-6 was added into the formed solution. The mixed solution was heated to 100 °C for 6 h in drying oven, after which period, the temperature was raised 160 °C for 6 h. The impregnation and drying procedures were repeated twice using 66 % sucrose. After carbonization, the sample was heated to 900 °C for 7 h under helium flow. The final mesoporous carbon product was obtained using 2 mol/L of NaOH aqueous solution to remove the silica template.

Characterizations of KIT-6, KIT-6-NC, and KIT-6-C

The X-ray diffraction patterns was recorded on a Philips PW3040/60 automatic powder diffractometer using $CuK\alpha$ radiation ($\lambda = 0.1542$ nm) at 40 kV and 40 mA. The scans were recorded in the 2θ values between 0° and 5° with a step width of 0.014°.

The transmission electron microscopy (TEM) images were recorded on a JEOL-2100F TEM working at 200 kV. The samples were diluted in ethanol and sonicated for 10 min. The ethanol slurry was then dripped onto a *Cu* grid covered with a thin film of carbon.

Surface areas of the carbon materials were calculated using the multipoint Brunauer–Emmett–Teller (BET) equation from nitrogen adsorption–desorption isotherms measured at liquid nitrogen temperature (Quantachrome Autosorb-1). The pore-size distribution curves were obtained from the desorption branches using the non-local density functional theory (NLDFT) method, and the total pore volume values were estimated from the adsorbed amount at a relative pressure P/P_0 of 0.99.

X-ray photoelectron spectra (XPS) were recorded on an ESCALAB 250Xi spectrometer with an Al anode *Ka* radiation (1486.6 eV). Carbonaceous C1 s line (284.6 eV) was used as a reference to calibrate the binding energies.

The CO_2 adsorption–desorption isotherms were measured using the Quantachrome Autosorb-1 equipment at

0 and 25 °C. Prior to each adsorption experiment, the sample was degassed for 5 h at 200 °C to remove the guest molecules from the pores.

Results and discussion

Structural characterization

Figure 1 shows the XRD patterns of KIT-6, mesoporous carbon (KIT-6-C), and nitrogen-doped mesoporous carbon (KIT-6-CN) in the small angle region. It can be seen that the template has three obvious diffraction peaks, indicating that KIT-6 exhibits ordered mesoporous structure. The intensity of diffraction peaks for KIT-6-C and KIT-6-CN became weaker. For KIT-6-CN, the diffraction peaks shifted to slightly higher 2θ values, indicating that KIT-6-CN has smaller pore sizes than KIT-6. In comparison, KIT-6-C synthesized using sucrose as carbon source has larger pore sizes than those of KIT-6.

The nitrogen adsorption–desorption isotherms of the KIT-6, KIT-6-C, and KIT-6-CN, are given in Fig. 2. It is clear that the isotherms of the silica KIT-6 show typical type IV curves with a steep H_1 hysteresis loop within the relative pressure (P/P_0) range of ca. 0.63–0.82. Its BET specific surface area and pore volume are as large with values of 566 m^2/g and 0.77 cm^3/g, respectively. These results are consistent with those reported by Ryoo et al. [20, 22], indicating that the mesoporous silica template was successfully synthesized. From the nitrogen isotherms of KIT-6-C and KIT-6-CN shown in Fig. 2, it can be deduced that the two isotherms also exhibit type IV curves and H1

hysteresis. KIT-6-CN shows a different hysteresis loop compared to those of KIT-6 and KIT-6-C, which may be due to two possible reasons. First, the processors for KIT-6-C and KIT-6-CN are different. For KIT-6-C, sucrose was used as processor, while EDA were used as processors for KIT-6-CN. Sucrose and EDA may show different properties during the carbonization process. Second, the preparation methods for KIT-6-C and KIT-6-CN are different. For KIT-6-C, the sucrose solution and KIT-6 template were treated in oven at 100 °C for 6 h. While EDA and KIT-6 were heated at 90 °C for 6 h with stirring under reflux to induce polymerization of the precursor. These two reasons may lead to different pore structures. The surface area and total pore volume of KIT-C are 740 m^2/g and 0.88 cm^3/g, and the corresponding values for KIT-6-CN are 587 m^2/g and 0.91 cm^3/g, respectively. The pore-size distribution is deduced using NLDFT method from adsorption isotherms, which allows for an accurate pore-size analysis over the complete range of micro- and mesopores. As shown in Fig. 2b, both KIT-6-C and KIT-6-CN possess pore-sizes of both microporous and mesoporous ranges. The micropores may result from the removal of the silica walls [21], and the mesopores may be due to the corresponding ordered structure of KIT-6. The micropores of both samples are centered around 1.7 nm, while their mesoporous sizes are 8.7 and 6.3 nm, respectively.

The structure and morphology of KIT-6-C and KIT-6-CN are also characterized by TEM. As shown in Fig. 3, both samples exhibit well-ordered mesopores with 3D porous network, although intensities of XRD diffraction peaks of carbon materials are weaker than that of the KIT-6 template as shown in Fig. 1. Thus, it can be concluded that both the nitrogen-doped and undoped mesoporous carbons with 3D porous network have been successfully synthesized using the hard template route.

Table 1 also gives the results of elemental analysis of KIT-6-CN. The contents of carbon, nitrogen, hydrogen, and silicon of KIT-6-CN are 76.5, 15.9, 4.2, and 1.6 wt%, respectively, which indicate that nitrogen has been effectively introduced into the mesoporous carbon. It should be noted that in previous studies, Vinu [18] and Li [21] et al. claimed that carbon nitrides (C_3N_4) were synthesized using EDA and CTC as carbon and nitrogen sources. However, our results indicate that the carbon content of the obtained product is much higher than that of C_3N_4, while the nitrogen content is much lower than that of C_3N_4. Furthermore, the synthesized materials are black in color, while it is known that C_3N_4 is yellow in color. Hence, the synthesized materials should be named as nitrogen-doped mesoporous carbon (KIT-6-CN) rather than C_3N_4 [23].
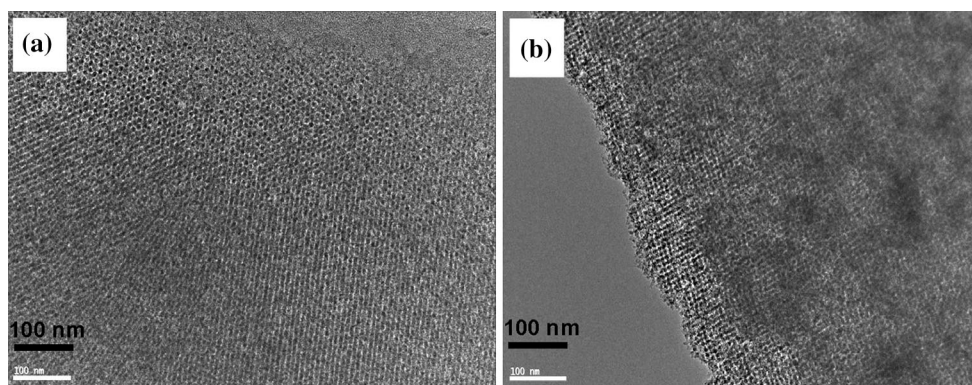
To investigate the chemical state of the doped nitrogen atoms, the KIT-6-C and KIT-6-CN samples were characterized by X-ray photoelectron spectroscopy (XPS). For
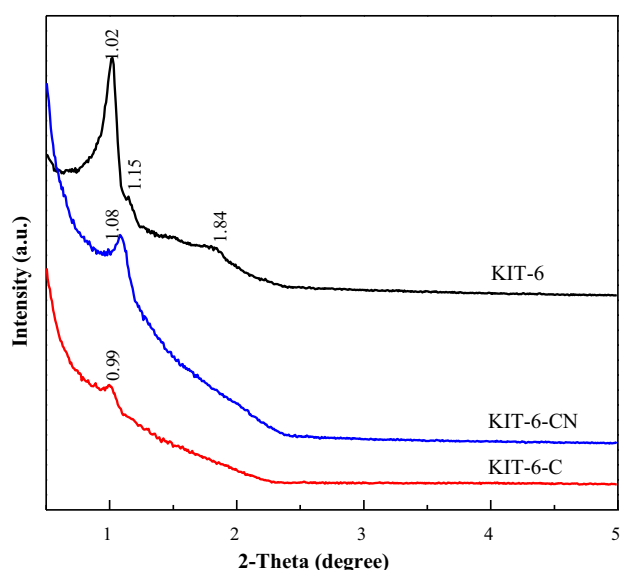
Fig. 1 XRD patterns of KIT-6, KIT-6-C, and KIT-6-CN
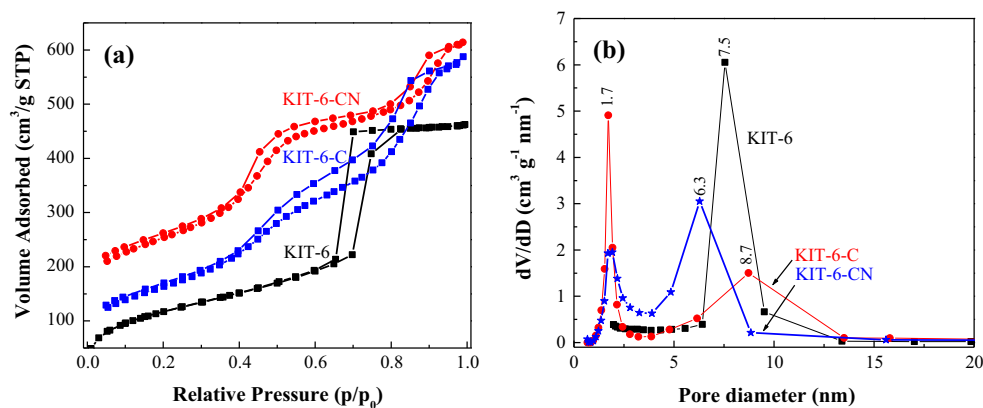
Fig. 2 **a** N$_2$ isotherms and **b** pore-size distributions of KIT-6, KIT-6-C, and KIT-6-CN

Fig. 3 TEM images of **a** KIT-6-C and **b** KIT-6-CN

Table 1 Textural properties of the prepared KIT-6, KIT-6-CN, and KIT-6-C

Sample	Surface area[a] (m^2/g)	Pore volume[b] (cm^3/g)	Average pore-size[c] (nm)	Elemental analysis[d] C (%) N (%) H (%) Si (%)
KIT-6	566	0.77	7.3	
KIT-6-C	740	0.88	1.7, 8.7	90.5, 0, 5.3, 2.0
KIT-6-CN	587	0.91	1.7, 6.3	76.5, 15.9, 4.2, 1.6

[a] The surface area was calculated using the BET method, $p/p_0 = 0.05–0.3$

[b] Total pore volume, $p/p_0 = 0.99$

[c] Determined from desorption branch according to non-local density functional theory (NLDFT) method

[d] Determined by elemental analyzer for C, N, and H, and determined by TGA for Si

KIT-6-C, no nitrogen signal was observed (the spectrum is not shown here), since the carbon precursor sucrose does not contain nitrogen content. For KIT-6-CN, C, N, and O signals were observed as shown in Fig. 4a. The O signal may be from the trace SiO$_2$ and the contaminant on sample surface. Figure 4b shows the XPS spectrum in N1 s region which can be deconvoluted into three peaks centered at 398.1, 399.8, and 400.4 eV. These three peaks are corresponding to different types of nitrogen species, i.e., pyridinic-type nitrogen, pyrrolic-type nitrogen, and quaternary nitrogen, respectively. The strong peaks at 398.1 and 399.8 eV indicate that most nitrogen atoms are pyridinic-type nitrogen and pyrrolic-type nitrogen species. It has been reported that pyrrolic-type nitrogen species favor the CO$_2$ capture performance of carbon [9, 24]. Therefore, KIT-6-CN is expected to possess better CO$_2$ capture performance than the KIT-6-C.
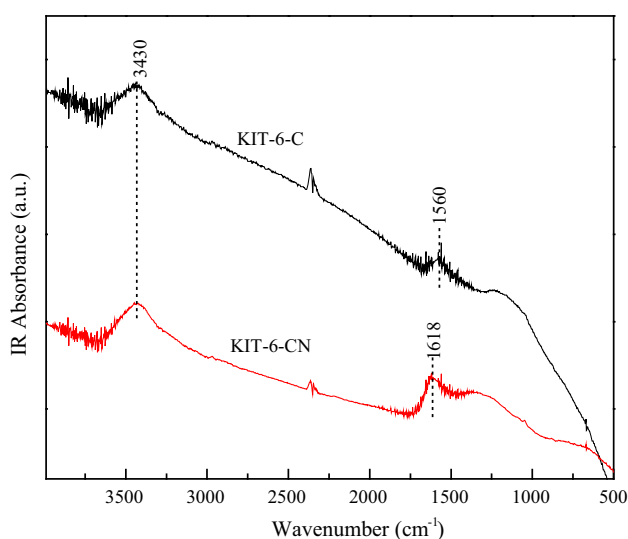
The FTIR spectra of KIT-6-C and KIT-6-CN are shown in Fig. 5. For KIT-6-C, the band at 1560 cm^{-1} is related to C–C stretching of aromatic ring structures, and the band at 3430 cm^{-1} is attributed to O–H stretching vibration of absorbed water molecules. For KIT-6-CN, a strong band at 1618 cm^{-1} can be ascribed to N–H deformation vibration, suggesting that the KIT-6-CN is mainly composed of pyridinic-type and pyrrolic-type nitrogen species.
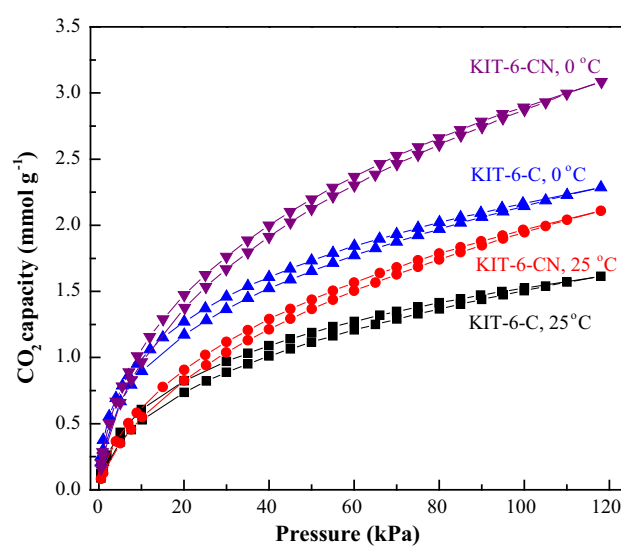
CO$_2$ adsorption test

The CO$_2$ capture performances of the obtained carbon materials were also tested. The CO$_2$ adsorption–desorption
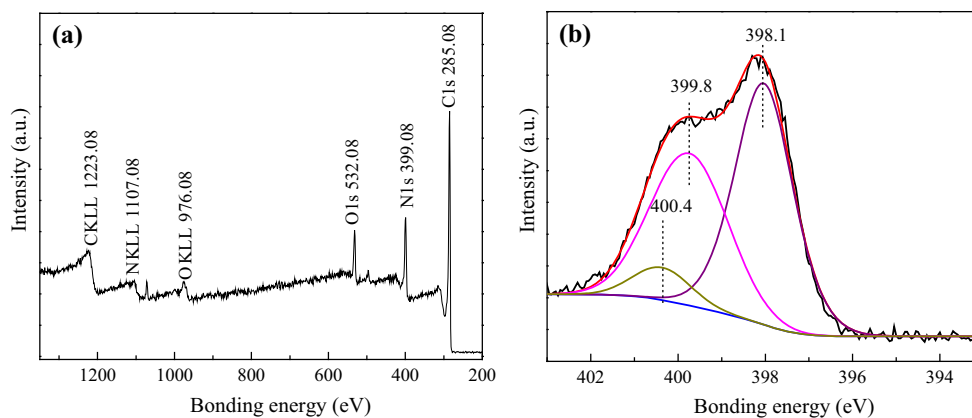
Fig. 4 XPS spectra of the KIT-6-CN

Fig. 5 FTIR spectra of the KIT-6-C and KIT-6-CN

Fig. 6 CO_2 absorption–desorption isotherms of KIT-6-C and KIT-6-CN at 25 and 0 °C

isotherms of KIT-6-C and the KIT-6-CN at 25 and 0 °C are shown in Fig. 6. Apparently, the CO_2 uptake of KIT-6-CN is higher than that of KIT-6-C almost in all pressure ranges at 25 °C. It can reach 2.11 mmol/g at ~120 kPa, while KIT-6-C can only adsorb 1.62 mmol/g CO_2 at the same pressure. When the temperature was decreased to 0 °C, the CO_2 capture performances of both samples were greatly improved. For example, the CO_2 uptake of the KIT-6-CN at 0 °C can reach 3.09 mmol/g which is 1.46 times of that at 25 °C. This indicates that the adsorption of CO_2 on carbon is mainly attributed to physical adsorption, and that lower temperature can improve the CO_2 capture performance. As is known to all, the interaction forces between carbon dioxide and sorbent surface are the weak van der Waals forces during the physisorption. When the temperature becomes higher, the thermal motion of the CO_2 molecules is accelerated; therefore, it is detrimental to the

adsorption. While it is also well known that gas uptake by physisorption is related to the porous texture of sorbents, as shown in Table 2, however, KIT-6-CN shows a similar porous texture as that of KIT-6-C. Then the superior CO_2 capture capacities of KIT-6-CN may be due to the nitrogen-doped species, the existence of which has been proven by XPS and FTIR analyses (Figs. 4, 5). It has been known that the nitrogen-doped atoms can change the chemical state of carbon materials and then improve the CO_2 capture performance of carbon materials [9].

Recently, Xu et al. reported some nitrogen-doped porous carbons synthesized using metal-organic frameworks (MOFs) [25, 26] as precursors. These carbons with high surface areas show ultrahigh CO_2 capture capacities which can reach 5.7 mmol/g at 277 K, which can be attributed to the dominant presence of micropores. For KIT-6-C and

Table 2 CO_2 capture capacities of KIT-6-CN and KIT-6-C at 25 and 0 °C

Sample	CO_2 uptake (mmol/g)	
	25 °C	0 °C
KIT-6-C	1.62	2.29
KIT-6-CN	2.11	3.09
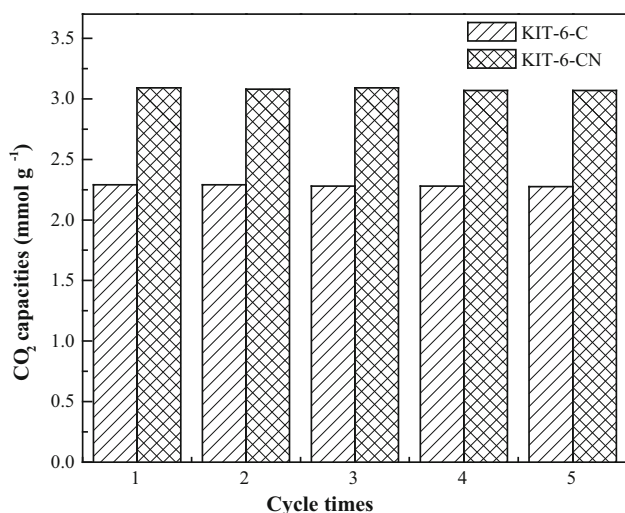
Fig. 7 Cyclic CO_2 absorption performances of KIT-6-C and KIT-6-CN at 0 °C

KIT-6-CN, the mesopores are dominant as shown in Fig. 2. This explains why they show lower CO_2 capture capacities.

The reversible nature of CO_2 capture performance on KIT-6-C and KIT-6-CN at 0 °C was also tested for five cycles. As shown in Fig. 7, the adsorption capacities for the five cycles did not show noticeable changes, indicating that both KIT-6-C and KIT-6-CN have good recyclability. Sethia et al. [27] also demonstrated that nitrogen-doped carbons show remarkable stability for CO_2 capture. This agrees well with our results. The good recyclability will improve the feasibility of these carbon materials for applications in CO_2 capture.

Conclusions

In summary, mesoporous nitrogen-doped carbon material (KIT-6-CN) has been successfully synthesized using *Ia3d* silica KIT-6 as a hard template, and CTC and EDA as precursors via a pyrolyzing process. KIT-6-CN has a relatively high BET surface area of 587 m^2/g and a pore volume of 0.91 cm^3/g. The CO_2 adsorption–desorption isotherms show that the adsorption capacities of KIT-6-CN at 25 and 0 °C are 2.11 and 3.09 mmol/g, respectively,

which are superior to those of the pure carbon materials with analogous mesostructures. This can be attributed to the doped alkaline nitrogen group into the carbon framework.

References

1. Kamarudin KSN, Alias N (2013) Adsorption performance of MCM-41 impregnated with amine for CO_2 removal. Fuel Process Technol 106:332–337
2. Song C (2006) Global challenges and strategies for control, conversion and utilization of CO_2 for sustainable development involving energy, catalysis, adsorption and chemical processing. Catal Today 115:2–32
3. Yu KMK, Curcic I, Gabriel J, Tsang SCE (2008) Recent advances in CO_2 capture and utilization. Chemsuschem 1:893–899
4. Cui S, Cheng WW, Shen XD, Fan MH, Russell A, Wu ZW, Yi XB (2011) Mesoporous amine-modified SiO_2 aerogel: a potential CO_2 sorbent. Energy Environ Sci 4:2070–2074
5. Yao M, Dong Y, Feng X, Hu X, Jia A, Xie G, Hu GS, Lu J, Luo M, Fan M (2014) The effect of post-processing conditions on aminosilane functionalization of mesocellular silica foam for post-combustion CO_2 capture. Fuel 123:66–72
6. Yao M, Dong Y, Hu X, Feng X, Jia A, Xie G, Hu GS, Lu J, Luo M, Fan M (2013) Tetraethylenepentamine-modified silica nanotubes for low-temperature CO_2 capture. Energy Fuels 27:7673–7680
7. Ma L, Bai R, Hu GS, Chen R, Hu X, Dai W, Dacosta HFM, Fan M (2013) Capturing CO_2 with amine-impregnated titanium oxides. Energy Fuels 27:5433–5439
8. Feng XX, Hu GS, Hu X, Xie GQ, Xie YL, Lu JQ, Luo MF (2013) Tetraethylenepentamine-modified siliceous mesocellular foam (MCF) for CO_2 capture. Ind Eng Chem Res 52:4221–4228
9. Liu L, Deng QF, Hou XX, Yuan ZY (2012) User-friendly synthesis of nitrogen-containing polymer and microporous carbon spheres for efficient CO_2 capture. J Mater Chem 22:15540–15548
10. An HB, Yu MJ, Kim JM, Jin M, Jeon JK, Park SH, Kim SS, Park YK (2012) Indoor formaldehyde removal over CMK-3. Nanoscale Res Lett 7:7–12
11. Xia Y, Mokaya R (2004) Synthesis of ordered mesoporous carbon and nitrogen-doped carbon materials with graphitic pore walls via a simple chemical vapor deposition method. Adv Mater 16:1553–1558
12. Fang B, Kim JH, Kim M-S, Yu J-S (2013) Hierarchical nanostructured carbons with meso macroporosity: design, characterization, and applications. Acc Chem Res 46:1397–1406
13. Xia Y, Yang Z, Mokaya R (2010) Templated nanoscale porous carbons. Nanoscale 2:639–659
14. Sun J-K, Xu Q (2014) Functional materials derived from open framework templates/precursors: synthesis and applications. Energy Environ Sci 7:2071–2100
15. Zelenak V, Badanicova M, Halamova D, Cejka J, Zukal A, Murafa N, Goerigk G (2008) Amine-modified ordered mesoporous silica: effect of pore size on carbon dioxide capture. Chem Eng J 144:336–342

16. Zelenak V, Halamova D, Gaberova L, Bloch E, Llewellyn P (2008) Amine-modified SBA-12 mesoporous silica for carbon dioxide capture: effect of amine basicity on sorption properties. Microporous Mesoporous Mater 116:358–364

17. Zhao C, Chen X, Zhao C (2009) CO_2 absorption using dry potassium-based sorbents with different supports. Energy Fuels 23:4683–4687

18. Vinu A (2008) Two-dimensional hexagonally-ordered mesoporous carbon nitrides with tunable pore diameter, surface area and nitrogen content. Adv Funct Mater 18:816–827

19. Deng Q-F, Liu L, Lin X-Z, Du G, Liu Y, Yuan Z-Y (2012) Synthesis and CO_2 capture properties of mesoporous carbon nitride materials. Chem Eng J 203:63–70

20. Kleitz F, Choi SH, Ryoo R (2003) Cubic *Ia3d* large mesoporous silica: synthesis and replication to platinum nanowires, carbon nanorods and carbon nanotubes. Chem Commun 7:2136–2137

21. Li Q, Yang JP, Feng D, Wu ZX, Wu QL, Park SS, Ha CS, Zhao DY (2010) Facile synthesis of porous carbon nitride spheres with hierarchical three-dimensional mesostructures for CO_2 capture. Nano Res 3:632–642

22. Choi DH, Ryoo R (2010) Template synthesis of ordered mesoporous organic polymeric materials using hydrophobic silylated KIT-6 mesoporous silica. J Mater Chem 20:5544–5550

23. Thrower PA (2004) What's in a name? Carbon 42:2367–2368

24. Liu L, Deng QF, Ma TY, Lin XZ, Hou XX, Liu YP, Yuan ZY (2011) Ordered mesoporous carbons: citric acid-catalyzed synthesis, nitrogen doping and CO_2 capture. J Mater Chem 21:16001–16009

25. Aijaz A, Fujiwara N, Xu Q (2014) From metal organic framework to nitrogen-decorated nanoporous carbons: high CO_2 uptake and efficient catalytic oxygen reduction. J Am Chem Soc 136:6790–6793

26. Aijaz A, Akita T, Yang H, Xu Q (2014) From ionic-liquid@ metal-organic framework composites to heteroatom-decorated large-surface area carbons: superior CO_2 and H_2 uptake. Chem Commun 50:6498–6501

27. Sethia G, Sayari A (2014) Nitrogen-doped carbons: remarkably stable materials for CO2 capture. Energy & Fuels 28:2727–2731